Journal of Power Sources 195 (2010) 104–110

Contents lists available at ScienceDirect

Journal of Power Sources

journal homepage: www.elsevier.com/locate/jpowsour

Evaluation of hydrogen and methanol fuel cell performance of sulfonated diels alder poly(phenylene) membranes

Ronald J. Stanis[a,*], Melissa A. Yaklin[a], Chris J. Cornelius[a,1], Tsutomu Takatera[b], Akimasa Umemoto[b], Andrea Ambrosini[a], Cy H. Fujimoto[a]

[a] Fuels and Energy Transitions, Sandia National Laboratories, Albuquerque, NM 87185, USA
[b] SHARP Corporation 2613-1, Ichinomoto-cho, Tenri, Nara 632-8567, Japan

ARTICLE INFO

Article history:
Received 10 June 2009
Accepted 23 June 2009
Available online 2 July 2009

Keywords:
Sulfonated diels alder poly(phenylene) (SDAPP)
Fuel cell
Proton conductivity
Hydrogen
Methanol

ABSTRACT

Hydrogen fuel cell performance of sulfonated diels alder poly(phenylene) (SDAPP) with IECs $\geq$ 1.8 meq g^{-1} is comparable to Nafion 212 under fully humidified conditions at 80 °C. However, as relative humidity is reduced, performance loss is substantial for SDAPP when compared to Nafion 212. This loss can be attributed to the large drop in proton conductivity in SDAPP as relative humidity is reduced; the proton conductivity of SDAPP with an IEC of 2.3 meq g^{-1} dropped from 0.117 S cm^{-1} to 0.001 S cm^{-1} as the relative humidity was reduced from 100% to 25% at 80 °C. Methanol fuel cell experiments using 3 M methanol result in a 60 mV performance improvement at 25 mA cm^{-2} when using SDAPP with an IEC of 1.2 meq g^{-1} instead of Nafion 212. This improvement is due to lower methanol permeability of SDAPP (1.4 meq g^{-1}) over Nafion 212, with SDAPP films having methanol permeabilities less than 25% of Nafion 212.

1. Introduction

Polymer electrolyte membrane fuel cells (PEMFCs) are considered excellent candidates for power sources which produce electricity for vehicles and portable electronics. Their high power density and ability to rapidly refuel provide significant advantages over battery systems. Large systems such as those considered for vehicles use hydrogen as the fuel because of the large power densities achieved (>700 mW cm^{-2} at >0.65 V) [1–4]. Sulfonated fluoropolymers such as Nafion serve as current state of the art PEM materials, due to low water uptake, high proton conductivity, chemical durability, and good fuel cell performance under specific conditions (fully humidified, 80 °C) [5]. To achieve optimal performance using sulfonated fluoropolymers, humidifiers are required which add undesired cost, weight, and volume to the hydrogen fuel cell system. A major research effort in the field of hydrogen fuel cells is focused on developing new PEMs, including acid-functionalized fluorinated, partially perfluorinated, and hydrocarbon polymers that can conduct protons at elevated temperatures and low relative humidity [5–7]. New PEMs need to be inexpensive because currently available perfluorinated polymers, such as Nafion, are considered prohibitively expensive [8].

Lower power density direct methanol fuel cells (DMFCs) have attracted interest as battery alternatives for mobile applications such as phones, mp3 players, and laptops because the use of methanol allows for simplified storage and refilling of the high energy density liquid fuel [9–11]. Direct methanol fuel cells suffer from lower volumetric power densities due to the slow reaction kinetics of methanol oxidation and the catalyst-poisoning effect of fuel crossover [9–11]. Fuel crossover also results in decreased fuel efficiency as the methanol that is oxidized at the cathode does not contribute to the power of the fuel cell. To reduce fuel crossover, thicker membranes are used and the concentration of methanol in the fuel is reduced to 0.5–2 M. Thicker membranes increase the volume of the fuel cell and the ionic resistance of the membrane, while low concentrations reduce the energy density of the fuel, adversely impacting one of the benefits of using DMFCs. A major research effort for DMFCs is to develop new thin PEMs which have very low methanol permeability but can still have high proton conductivity [10–18].

We have previously reported on sulfonated diels alder poly(phenylene) (SDAPP), which has shown potential as a candidate PEM material for hydrogen and methanol fuel cells due to its high proton conductivity and low methanol permeability [19,20]. The structure of SDAPP is presented in Fig. 1. For every repeat unit there are six potential pendent phenyl groups for attachment of

* Corresponding author. Present address: Office of Technology and Innovation, Gas Technology Institute 1700 South Mount Prospect Road, Des Plaines, IL 60018, USA. Tel.: +1 847 620 9460.
E-mail address: Ron.Stanis@gastechnology.org (R.J. Stanis).
[1] Present address: Department of Chemical Engineering, Virginia Tech, Blacksburg, VA 24061, USA.

0378-7753/$ – see front matter © 2009 Elsevier B.V. All rights reserved.
doi:10.1016/j.jpowsour.2009.06.082

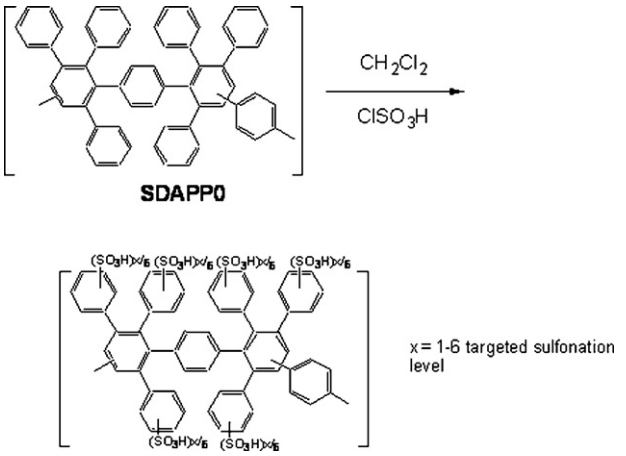

Fig. 1. Sulfonation scheme and structure of SDAPP.

a sulfonic acid group. The degree of sulfonation (and resulting ion exchange capacity, IEC meq g^{-1}) can be controlled by increasing the ratio of chlorosulfonic acid to the parent polymer during synthesis. The nomenclature used in this report refers to the targeted sulfonation level. For example, SDAPP2 implies that chlorosulfonic acid and the parent polymer were added in the appropriate ratio to target two sulfonic acids per repeat unit; however the actual sulfonation efficiency is less than 100% [19]. The objective of this work is to compare the performance of hydrogen and methanol fuel cells utilizing SDAPP membranes with varying degrees of sulfonation.

2. Experimental

2.1. Materials

The synthesis of diels alder poly(phenylene) and subsequent sulfonation was repeated according to methods described in the literature [19,21]. Films were cast from a solution of 5 wt.% polymer dissolved in dimethylacetamide (DMAc) onto a bordered glass plate. The plate was placed into a vacuum oven at 40 °C overnight. After 12 h, the temperature was increased and held for 2 h each at 60 °C and 80 °C. The dry films were then boiled for 1 h successively in 1 M H_2SO_4 and DI water, to exchange the Na^+ ions presenting the film to H^+ and to ensure removal of any residual dimethylacetamide. Resulting films had a room temperature water-swelled thickness of 2.65 mil to match that of Nafion 212.

Gas diffusion electrodes were prepared by spray coating a catalyst ink solution onto microporous 35BC paper electrodes (SGL carbon), using a computer controlled X-Y system and syringe pump. Hydrogen fuel cell experiments utilized anodes and cathodes prepared with 0.4 mg Pt cm^{-2} (20% Pt on Vulcan XC72, E-tek) mixed with 25 wt.% Nafion solution purchased from Aldrich. Cathodes for methanol experiments contained an increased catalyst loading of 1 mg Pt cm^{-2}. Anodes for methanol experiments utilized 4 mg PtRu cm^{-2} (50:50 Pt:Ru black, unsupported, E-tek). Nafion 212 was purchased from Ion Power and was pretreated by boiling for 1 h each in solutions of 3% H_2O_2, DI water, 1 M H_2SO_4 and DI water. After pretreatment the Nafion 212 was stored in DI water in a sealed container in the dark.

2.2. MEA preparation

Membrane electrode assemblies (MEAs) were prepared by hot pressing. Conditions were 145 °C and 2000 lbs of force for 6 min for Nafion MEAs. For SDAPP MEAs 2000 lbs of force were applied as the plates were heated from 25 °C to 120 °C at a rate of 12 °C min^{-1} for a total of 10 min.

2.3. Characterization

2.3.1. Weight and volume-based IEC

Weight based ion exchange capacity (IEC_w) in meq g^{-1} was determined by titration of acidified films [19]. Films were cut out using a cork bore with a diameter of 20 mm and were soaked in 50 ml of 1 M Na_2SO_4 for 24 h. The solutions were then titrated with 2 mM NaOH until an end point of pH 7 was reached.

The thickness (t) and diameter (d) of the films were measured in both the wet and dry state and were used to determine volume by Eq. (1):

$$V = \pi\left(\frac{d}{2}\right)^2 t \tag{1}$$

Volume-based ion exchange capacity (IEC_{vol}) in meq cm^{-3} was calculated using Eq. (2):

$$IEC_{vol,(dry\ or\ wet)} = \frac{[\text{mmol } H^+]}{[\text{Volume}_{dry\ or\ wet}]} \tag{2}$$

2.3.2. Conductivity in air

Proton conductivity experiments in humidified air were performed by electrochemical impedance spectroscopy (EIS) using a Solartron 1260 frequency response analyzer and a Solartron 1287 potentiostat. The membranes were first dried on a vacuum plate for 30 min, and then mounted in a two point-probe "window cell" [19] which was placed in a temperature and humidity controlled chamber. The films were equilibrated at each humidity for at least 3 h starting with the lowest relative humidity and stepping up, before conductivities were measured. A Labview program using feedback from a Vaisala humidity probe was used to blend humidified and dry air feeds to obtain desired humidities. The EIS measurements were taken over a frequency range of 1 Hz to 300 kHz. The real (Z') and imaginary (Z'') impedance components were plotted and the resistance (R) was taken as the value of Z' when extrapolating the line to $Z'' = 0$. The conductivity (σ) of the sample was then calculated using Eq. (3):

$$\sigma = \frac{d}{Rwt} \tag{3}$$

where d is the distance between the electrodes, w is the width of the sample and t is the thickness of the sample. A series of measurements were taken for each data point and the average resistance was used to calculate the conductivity.

2.3.3. Conductivity in methanol solutions

The proton conductivity of the films was also measured in solutions of methanol. The films were placed in the same window cell as described in Section 2.3.2 but the hardware was immersed in baths of methanol solutions (0, 0.5, 1, 2, and 3 M) at 60 °C. EIS was performed to determine the proton conductivity.

2.3.4. Methanol permeation

Methanol permeability was determined using a membrane-separated diffusion cell as described in a previous report [20]. Each film separated 20 ml of water and 20 ml of 1 M methanol. An HPLC pump was used to circulate the water side at 7 ml min^{-1} through a Waters 2414 refractive index detector to determine the methanol concentration. Measurements were taken at 40, 60 and 80 °C. The permeability, DH (the product of the diffusion coefficient, D, and the solubility, H), can be calculated from the following equations:

$$-DH \cdot \chi \cdot t = \ln\left(\frac{c_{SR} - c_{WR}}{c^o_{SR} - c^o_{WR}}\right) \tag{4}$$

$$\chi = \frac{A}{l}\left(\frac{1}{V_L} + \frac{1}{V_R}\right) \tag{5}$$

Table 1
Ion exchange capacities of Nafion212 and SDAPP by mass and volume (dry and wet) and dissolved membrane mass fractions.

Membrane	IEC (meq g^{-1})	$IEC_{vol.dry}$ (meq cm^{-3})	$IEC_{vol.wet}$ (meq cm^{-3})	Water uptake (%)	Mass% dissolved[a]
Nation 212	0.92	1.8	1	38	100
SDAPP1	0.72	0.82	0.73	18	1.5
SDAPP2	1.2	1.4	1	29	2.5
SDAPP3	1.7	2.0	1.2	55	100
SDAPP4	2.3	2.9	1.5	85	100

All membranes were boiled successively in 1 M H_2SO_4 and DI water. Uncertainty ±2% of value for IEC, ±4 of value for water uptake, based on average 3 samples.
[a] After 1 week in 0.50 mol fraction methanol at 80 °C; membranes which dissolved 100% did so within 4 h of start of experiment, uncertainty is ±0.5% based on 3 samples.

where c_{SR} and c_{WR} are the concentration of solute in the solute-rich and water-rich compartments at time t, c^o_{SR} and c^o_{WR} are the initial concentrations in the two compartments at time zero, A is the active area of transport, l is the thickness of the film, V_L is the volume of the solute-rich cell, and V_R the water-rich volume at time $t = 0$. The volumes of V_L and V_R are assumed to remain constant throughout the course of the experiment. A plot of $\ln[(c_{SR} - c_{WR})/(c^o_{SR} - c^o_{WR})]$ versus t yields a straight line with slope $-DH\cdot\chi$. Once χ is determined by measuring the geometry of the cell, the permeability of the membrane can be calculated.

2.3.5. Dissolution in a methanol solution

Each film was cut into squares of 5 cm^2 dried in a vacuum oven (80 °C) overnight, weighed, and placed into 50 cm^2 glass vials containing 40 ml of 0.5 mol fraction methanol and water (~17 M). The vials were capped tightly then placed in an oven at 80 °C for 1 week. The remains of the films were removed from the solutions, placed in a vacuum oven overnight and the % mass dissolved was determined by the change in mass. The experiment was performed in triplicate for each film composition.

2.3.6. Fuel cell testing

Membrane electrode assemblies with electrode geometric surface areas of 5 cm^2 were assembled into fuel cell hardware (Fuel Cell Technologies) and tested using Fuel Cell Technologies test stations. The load control, gas flows, humidifier temperatures, cell temperature, and backpressure were all controlled by the test stations. During hydrogen testing, gas flow rates of 200 sccm were used and backpressure of 20 psig was maintained. To vary the inlet relative humidity, the humidifier temperatures were controlled at 49, 64, 73, and 80 °C to achieve 25, 50, 75 and 100% RH, respectively, when the cell temperature was 80 °C. All MEAs were broken in for 24 h before testing by alternating half-hour constant voltage holds of 0.5 and 0.6 V when using H_2, and 0.25 and 0.35 V when using methanol. Polarization curves were measured by scanning the voltage from open circuit voltage (OCV) to 0.7 V with a step size of 0.01 V holding each step for 6 min before the data point was recorded. Below 0.7 V, a step size of 0.05 V was used down to 0.25 V, at which point the load was removed.

Methanol fuel cell testing was performed by pumping methanol to the anode at 1 ml min^{-1} with no backpressure. The methanol was preheated to the cell temperature before entering the cell. Air was fed to the cathode at 200 sccm and 15 psig backpressure. Polarization curves were measured by scanning from OCV to 0.4 V with a step size of 0.01 V, holding each step 6 min before each data point is collected. Below 0.4 V a step size of 0.02 V was used down to 0.1 V, at which point the load was removed.

3. Results and discussion

3.1. Ion exchange capacity as a function of mass and volume

The ion exchange capacity (IEC) of each membrane is listed in Table 1, including Nafion which serves as a reference. The IEC of Nafion is much lower than those of the highly sulfonated SDAPP materials due to the difference in molecular weight and density of the fluorinated straight chain versus the highly phenylated hydrocarbon polymers. Although ion content is generally measured by IEC in terms of weight [meq g^{-1}], recently [22,23] a nomenclature of acid per unit volume has been used. The unit of volume may be more relevant in terms of fuel cell properties since it describes the acid concentration in both wet and dry states. In the dry state, the $IEC_{vol.dry}$ is higher relative to IEC_{wt}, while in the wet state $IEC_{vol.wet}$ is lower than IEC_{wt}. Moreover, in the series there is a progressive drop in acid concentration from SDAPP1 to SDAPP4 between dry and wet states; SDAPP1 11%, SDAPP2 29%, SDAPP3 40%, SDAPP4 48%. This drop is due to the progressive swelling of the membrane as the ion content is increased (Table 1, water uptake); as the ion content approaches percolation the swelling becomes excessive. Since IEC by volume is a measure of proton concentration, in the wet state, absorbed water swells the polymer matrix which in effect reduces proton concentration compared to the dry state.

3.2. Conductivity

The effect of ion concentration and polymer morphology/functionalization can be readily observed by examining proton conductivity vs. relative humidity, Fig. 2. At 80 °C and 100% RH the $IEC_{vol.wet}$ of SDAPP1 (0.73 meq cm^{-3}) and SDAPP2 (1.0 meq cm^{-3}) are similar to Nafion 212 (1.0 meq cm^{-3}), however their proton conductivities are over an order of magnitude lower. This discrepancy between proton concentration and conductivity between SDAPP and Nafion is due to the fact that $IEC_{vol.wet}$ does not distinguish between strong/weak acids nor does it take into account ion channel tortuosity and connectivity. Nafion contains perfluoronated

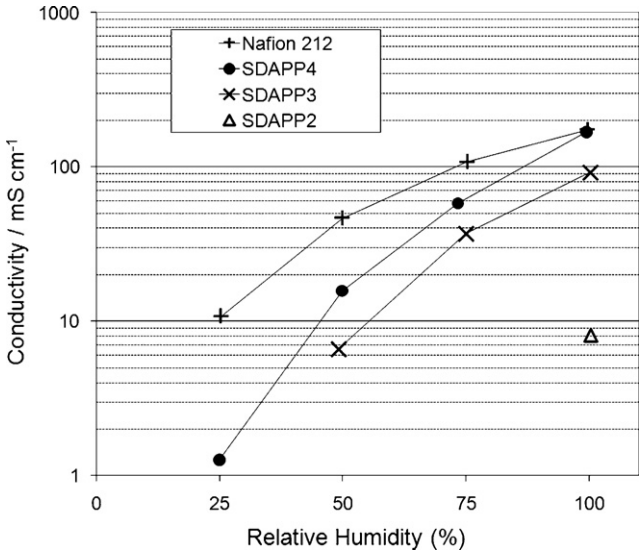

Fig. 2. Proton conductivity of membranes measured at various relative humidities in air at 20 psig and 80 °C using impedance spectroscopy.

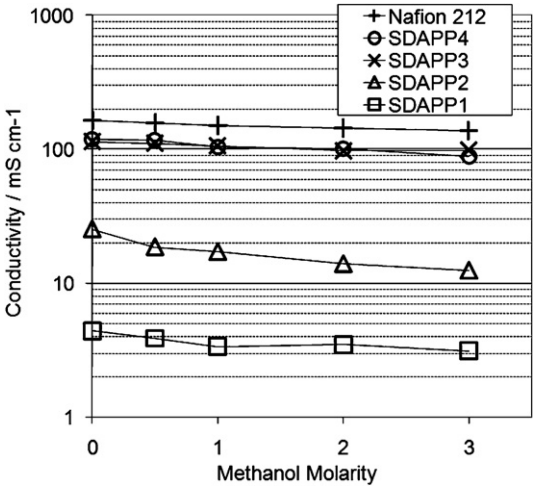

Fig. 3. Proton conductivity of membranes measured in methanol solutions at 60 °C using impedance spectroscopy.

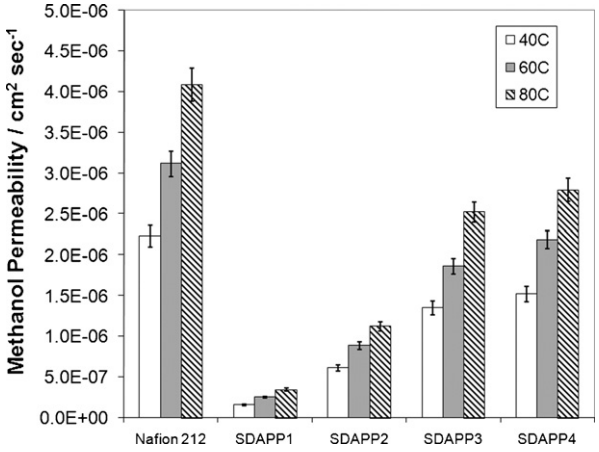

Fig. 4. Methanol permeability as a function of temperature for SDAPP samples and Nafion 212.

sulfonic acid which is stronger than aryl sulfonic acid [pKa −5 vs. −1, respectively], and studies by Kreuer [24] have shown that perfluoronated polymers exhibit enhanced phase separation (larger hydrophilic channels with more connectivity) compared to post-sulfonated hydrocarbons. Because of lower acid strength and higher tortuosity, higher SDAPP ion concentrations [≥1.0 meq cm^{-3}] are needed to obtain proton conductivities comparable to Nafion at 100% RH.

As the $IEC_{vol.wet}$ increases from 1.0 meq cm^{-3} (SDAPP2) to 1.2 meq cm^{-3} (SDAPP3) the proton conductivity at 80 °C and 100% RH increases dramatically from 8 mS cm^{-1} to 92 mS cm^{-1}. An increase in $IEC_{vol.wet}$ to 1.5 meq cm^{-3} (SDAPP4) offers an increase to 169 mS cm^{-1}. These values are substantially lower than values obtained in liquid water [20] at 80 °C (SDAPP1 27 mS cm^{-1}, SDAPP2 92 mS cm^{-1}, SDAPP3 161 mS cm^{-1}, SDAPP4 201 mS cm^{-1}). These differences in conductivity could be attributed to lower water content between vapor vs. liquid phase equilibrated membranes, as Nafion have been reported [25] to have lower values in the former.

As relative humidity decreases, the conductivities of SDAPP1 and SDAPP2 become highly resistive and therefore are not presented. For SDAPP3 and SDAPP4 the proton conductivity is measureable at low relative humidity, but the conductivity declines rapidly with decreasing relative humidity. This is further highlighted when comparing the % decrease of proton conductivity relative to conductivity at 100% RH. The conductivity of SDAPP4 drops by 66% at 75% RH, 87% at 50% RH and 99% at 25% RH, while Nafion observes losses only by 8, 72, and 94%, respectively. These sharp decreases in proton conductivity of SDAPP are not unexpected, since it is accepted that randomly sulfonated polymers lack the proper ion connectivity among acid groups for proton transport, which are further exasperated under partially hydrated conditions [26]. Recently, Kim [27] has reported dramatic decreases in proton conductivity as relative humidity falls in randomly sulfonated poly(arylene ether) compared to Nafion or ordered multi-block polymers, presumably due to poor phase connectivity of hydrophilic domains in the random system.

The effect of methanol concentration on the proton conductivity of SDAPP and Nafion membranes at 60 °C is presented in Fig. 3. As the methanol concentration increases from 0 M to 3 M, the conductivity of Nafion decreases from 164 mS cm^{-1} to 137 mS cm^{-1} and the conductivities of SDAPP4 and SDAPP3 decreases from160 mS cm^{-1} to 132 mS cm^{-1} and 114 to 98 mS cm^{-1}, respectively. These decreases are small and unlikely to greatly affect the performance of the methanol fuel cell. The consequence of increasing methanol concentration is much more severe for the films with lower IECs. The conductivity of SDAPP2 is halved from 25 mS cm^{-1} to 12 mS cm^{-1} when the concentration of methanol increases from 0 M to 3 M. It is thought that hydrocarbon membranes for DMFC applications may sacrifice proton conductivity for achieving low crossover [15]. The results presented in Fig. 3 call attention to the need to ensure that DMFC membranes retain acceptable proton conductivity at high methanol concentrations.

3.3. Methanol solubility

Siroma et al. studied the solubility of Nafion films in methanol solutions and found that Nafion can be highly soluble depending on methanol concentration and temperature [28]. The solubility became more pronounced at methanol mole fractions above 0.5 at temperatures below 65 °C. The solubility increased with temperature and became severe at 80 °C. The solubility of SDAPP and Nafion films under the harsh condition of 0.5 mol fraction methanol at 80 °C is presented in Table 1. This concentration was chosen because in a DMFC, water and methanol are required to be in at least a 50:50 ratio for the oxidation of methanol to occur with water, according to the reaction stoichiometry. The percent polymer dissolved was determined by the change in mass of the solid films after one week in the solutions. Within 4 h of the start of the experiment, Nafion 212, SDAPP3 and SDAPP4 had completely dissolved, while SDAPP1 and SDAPP2 films remained intact with only trace weight loss. These results suggest that SDAPP membranes could be highly stable DMFC membranes provided that the IEC is below a specified value.

3.4. Methanol permeability

The calculated methanol permeabilities for Nafion and SDAPP1–4 at 40 °C, 60 °C and 80 °C are presented in Fig. 4. The methanol permeability depends heavily on the IEC of the SDAPP membranes. At 80 °C the SDAPP3 and SDAPP4 films have methanol permeabilities about half that of Nafion 212. SDAPP2, which has a low degree of sulfonation, has a measured methanol permeability approximately one quarter that of Nafion 212. Permeability is the product of the diffusion coefficient and the solubility of methanol in the membrane. The decrease in methanol permeability with IEC is a trend typical of proton exchange membranes [18,29]. The additional sulfonic acid groups allow for increased water uptake which causes swelling of the membrane. This swelling opens up the channels allowing for higher methanol diffusion.

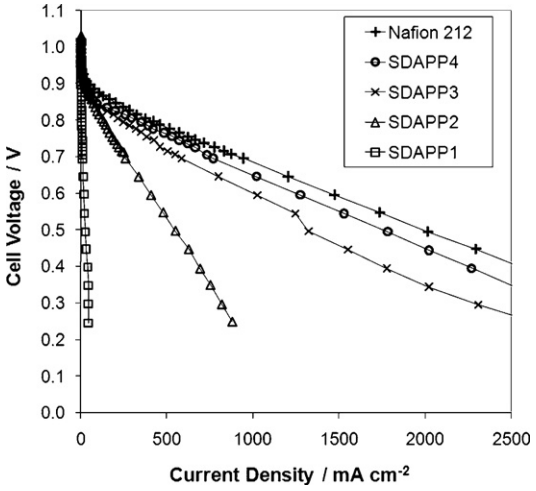

Fig. 5. H_2/O_2 polarization curves measured at 80 °C and 100% RH.

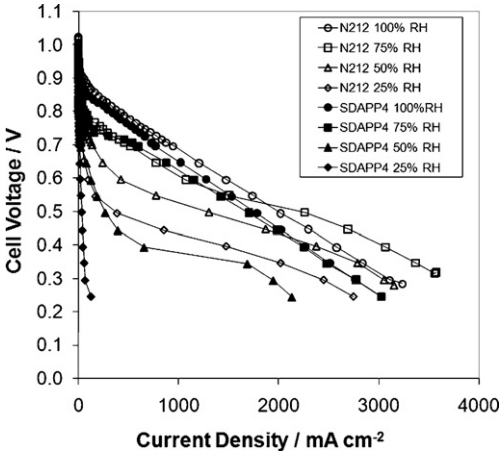

Fig. 7. H_2/O_2 polarization curves of SDAPP4 vs. Nafion212 measured at 80 °C at various RH.

3.5. Hydrogen fuel cell performance

A comparison of the fuel cell performance of MEAs utilizing Nafion and SDAPP1-4 membranes at 80 °C and 100% RH is presented in Fig. 5 for H_2/O_2 experiments and Fig. 6 for H_2/air experiments. It is clear that SDAPP1 and SDAPP2, which have very low IECs and proton conductivities, exhibit poor fuel cell performance. Using O_2 as the oxidant, the performance of SDAPP3 and SDAPP4 is slightly less than that of Nafion and is in agreement with the conductivity results as discussed in Section 3.1. Under these ideal conditions (100% RH and pure O_2) the performance of SDAPP4 is quite comparable to Nafion 212. At 0.65 V the MEA using SDAPP4 achieved 1020 mA cm^{-2}, just 15% less than the 1204 mA cm^{-2} achieved by the MEA using Nafion 212. The performance is comparable considering that Nafion 212 is a highly optimized 2nd generation commercially available polymer, and that SDAPP is not optimized and is produced at the laboratory scale. In Fig. 6, the fuel cell performance difference between SDAPP3, SDAPP4 and Nafion is much greater when using air as the oxidant as a result of mass transport effects. Despite these differences, the relative performance of SDAPP3 and SDAPP4 is comparable to Nafion at 100% RH using hydrogen fuel. Through optimization of the IEC, the membrane electrode assembly process, and the thickness of the membrane, the performance of SDAPP can be improved to rival that of Nafion under fully humidified conditions.

The hydrogen fuel cell performance of SDAPP4 and Nafion 212 at 80 °C under variable relative humidity conditions is presented in Fig. 7 using oxygen and Fig. 8 using air. When using pure oxygen, as the relative humidity of the inlet gases decreases, the current density achieved by the Nafion 212 MEA at 0.65 V drops from 1204 mA cm^{-2} to 55 mA cm^{-2}. These values result in performance losses of 36%, 80% and 95% (relative to current density at 100% RH) respectively for Nafion 212. While using air, the losses are very similar at 43%, 80% and 95% respectively for Nafion 212. These percent decreases in fuel cell performance under O_2, relative to performance at saturated conditions are strikingly similar to the percent decreases in proton conductivity as discussed in Section 3.2. Likewise, SDAPP4 experiences performance losses of 57%, 92% and 98% (relative to current density at 100%RH) which are strikingly similar to the to proton conductivity losses reported in Section 3.2. It can be concluded that the majority of the cell losses at low relative humidity are due to decreases in proton conductivity. Moreover, since the proton conductivity of SDAPP materials are highly diminished under low water contents, its fuel cell performance lags behind Nafion under medium to low relative humidity conditions. Although, post-sulfonated SDAPP does not meet one of the major qualifications required for alternative fuel cell membranes at low relative humidity, the good proton conductivity at high relative humidity does suggest that SDAPP could be consid-

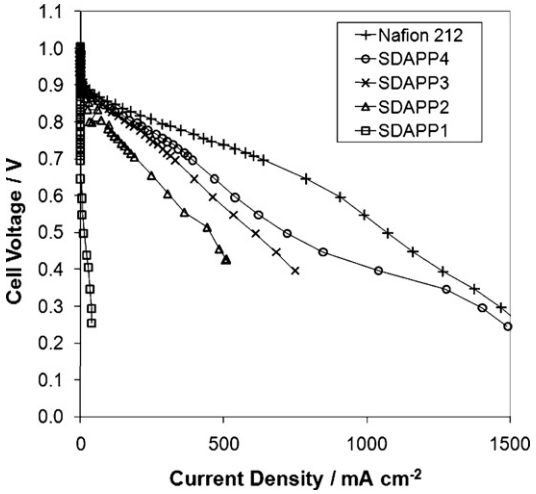

Fig. 6. H_2/air polarization curves measured at 80 °C and 100% RH.

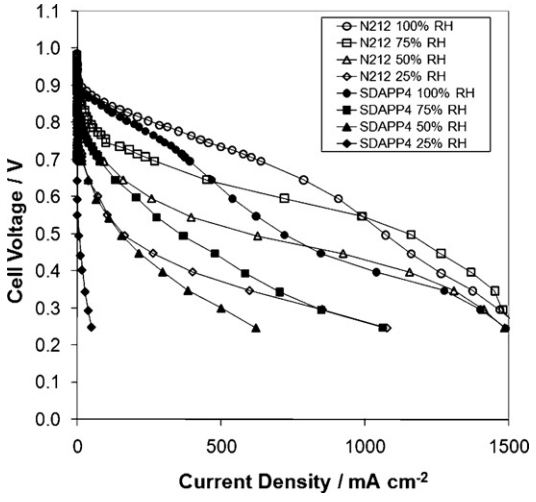

Fig. 8. H_2/air polarization curves of SDAPP4 vs. Nafion212 measured at 80 °C at various RH.

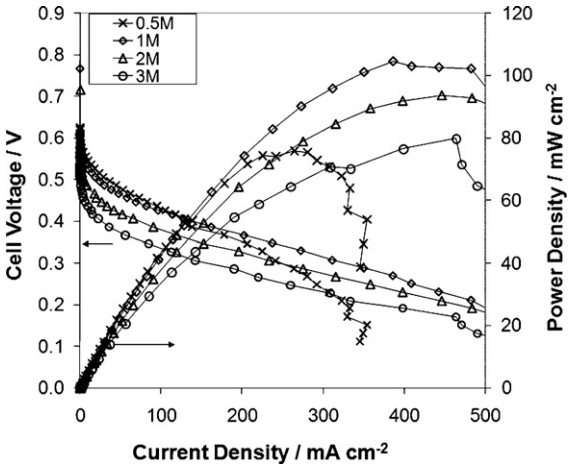

Fig. 9. Polarization curves for Nafion 212 measured at 80 °C, with 1 ml min^{-1} methanol fed to anode at 0 psig backpressure and 200 sccm of air fed to the cathode at 15 psig backpressure.

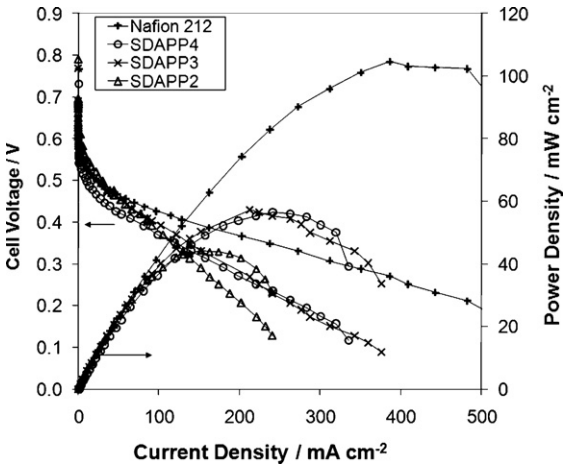

Fig. 10. Polarization curves for MEAs using chosen membranes measured at 80 °C, with 1 ml min^{-1} 1 M methanol fed to anode at 0 psig backpressure and 200 sccm of air fed to the cathode at 15 psig backpressure.

ered useful for other ion-exchange electrochemical processes such as chlor-alkali, electrodialysis, and redox flow batteries [30–32]. The fact that SDAPP materials are hydrocarbon based provides them with a significant cost advantage over Nafion [8]. A less expensive hydrocarbon membrane can significantly reduce the cost of a fuel cell system.

3.6. Direct methanol fuel cell performance

The convenience of using liquid methanol as a fuel allows for DMFCs to have a significant advantage over hydrogen fuel cells for portable electronic devices. Unfortunately, Nafion polymer electrolyte membranes suffer from high methanol crossover that negatively affects the fuel cell performance. The effect of increasing methanol feed concentration on the performance of a Nafion 212 DMFC MEA is presented in Fig. 9. A significant drop in operating voltage can be observed throughout the entire polarization curve as the concentration of methanol is increased from 0.5 M to 3 M, as the methanol that crosses over poisons the cathode catalyst [9–11]. The power densities drop more rapidly with increasing current densities when using 0.5 M fuel due to poor mass transfer of methanol to the anode catalyst in such a dilute fuel. For practical purposes the use of a low concentration fuel is not desired, as the total volume of fuel required for the system would be much higher relative to using a concentrated fuel. If the targeted application for the fuel cell system, such as a cell phone or laptop has volume constraints, a low concentration fuel would result in decreased run times between refueling.

Membrane electrode assemblies using SDAPP membranes of varying IECs were tested using methanol fuel cell conditions. Thin membranes (2.65 mil wet, room temperature) were chosen to maximize the effect of fuel crossover. Under these conditions, as methanol crossover is decreased through the use of a less permeable membrane, the effects are dramatic. The direct methanol fuel cell polarization curves for MEAs utilizing Nafion and SDAPP2, 3, and 4 membranes are presented in Figs. 10 and 11, for 1 M, and 3 M methanol fuels, respectively. Although membrane conductivity heavily influences the hydrogen fuel cell performance, it can be seen in Fig. 10 that proton conductivity becomes less important. Using 1 M fuel, the MEAs with highly conductive membranes have significantly higher maximum power densities, but these power densities are achieved at low voltages (< 0.25 V). Operation at higher cell voltages (> 0.4 V) is desired to obtain high thermodynamic or voltage efficiency. It is acknowledged that thermodynamic efficiency must be sacrificed somewhat to achieve high current densities. As a result, maximum Faradiac and overall DMFC efficiency can be achieved at lower voltages depending on the system [33,34]. When using the dilute 1 M fuel, there is no practical difference between membranes in power density in the high voltage, low current density region of the polarization curves (>0.4 V, <100 mA cm^{-2}). At higher current densities the effect of conductivity becomes apparent.

The performance results using 3 M methanol fuel are presented in Fig. 11. The increased methanol concentration results in an increased poisoning effect and power densities are reduced. The superior methanol blocking characteristics of the SDAPP2 MEA are evident in the results using 3 M methanol fuel, which show that while the performance of the Nafion 212, SDAPP3 and SDAPP4 membranes is heavily poisoned from the greater fuel crossover, the performance of the MEA using SDAPP2 remains quite good in the high voltage, low current density region. The performance of the SDAPP2 MEA does decrease with increasing methanol concentration; however the decreases are less dramatic. While using 3 M fuel the SDAPP2 MEA achieves 25 mA cm^{-2} at 0.46 V, a 50 mV drop compared to the 1 M fuel. At this same current density, the Nafion 212

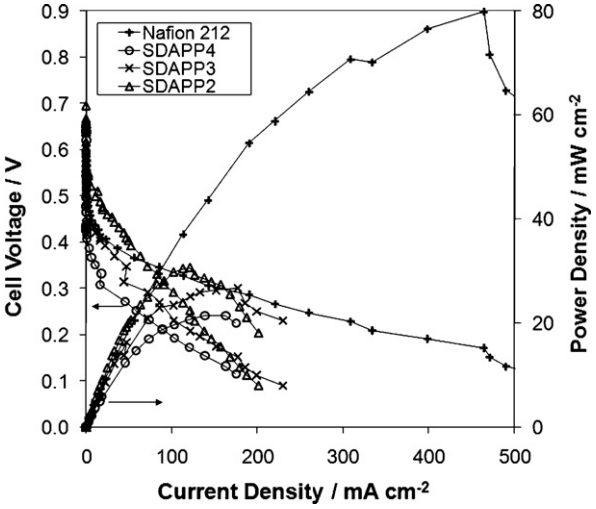

Fig. 11. Polarization curves for MEAs using chosen membranes measured at 80 °C, with 1 ml min^{-1} 3 M methanol fed to anode at 0 psig backpressure and 200 sccm of air fed to the cathode at 15 psig backpressure.

MEA operates at 0.4 V, which is nearly a 100 mV drop when compared to operation at 1 M. As a result, with 3 M fuel the SDAPP2 MEA achieves 25 mA cm^{-2} at a voltage 60 mV higher than that of the Nafion 212 membrane. Below voltages of 0.35 V, the Nafion 212 MEA outperforms the SDAPP2 MEA because the SDAPP2 membrane has low proton conductivity as discussed in Section 3.1. In Section 3.4 it was observed that the methanol permeability of SDAPP3 and SDAPP4 is approximately half that of Nafion, while the methanol permeability of SPAPP2 is approximately one quarter that of Nafion. In the polarization curves displayed in Fig. 11 only SDAPP2 shows a significant reduction in the methanol crossover poisoning effect while SDAPP3 and SDAPP4 do not. Therefore it can be concluded that reductions in methanol permeability on the order of 75% are required to mitigate the methanol crossover poisoning effect in the DMFC. For a practical DMFC application the IEC of SDAPP could be tailored to reduce crossover and attain a targeted power density by balancing the methanol permeability and proton conductivity properties.

4. Conclusions

The performance of SDAPP as PEM materials for hydrogen and methanol fuel cells was determined through the consideration of a number of characteristics. The proton conductivity of SDAPP was determined in varying concentrations of methanol and in varying relative humidity environments. SDAPP membranes are much more dependent on humidity than Nafion membranes, which results in reduced hydrogen fuel cell performance relative to Nafion at low relative humidity. Although the SDAPP membranes are comparable to Nafion at saturated conditions, their poor performance at low relative humidity will limit their consideration as replacements for Nafion in hydrogen fuel cells using dry fuels. The lower cost of the hydrocarbon based SDAPP makes the polymer an economical alternative to perflourinated Nafion especially in cases where high relative humidity is used.

While SDAPP2 (IEC = 1.2 meq g^{-1}) had low proton conductivity in methanol solutions at 60 °C, its methanol permeability was one quarter that of Nafion 212. This decreased methanol permeability resulted in superior fuel cell performance using 3 M fuel at voltages above 0.35 V. Below this voltage region the low proton conductivity of SDAPP2 served as a disadvantage. Based on these results it can be concluded that SDAPP is a potentially suitable alternative to Nafion in DMFCs. Future studies should focus on optimizing the IEC between 1.2 and 1.8 meq g^{-1} in order to maximize conductivity while maintaining low methanol permeability.

Acknowledgments

We would like to thank the Sharp Corporation for partial funding support of this research under CRADA No. SC05/01712. Sandia National Laboratories is a multi-program laboratory operated by Sandia Corporation, a Lockheed Martin Company, for the United States Department of Energy's National Nuclear Security Administration under contract DE-AC04-94AL-85000.

References

[1] H.A. Gasteiger, S.S. Kocha, B. Sompalli, F.T. Wagner, Applied Catalysis B: Environmental 56 (1–2) (2004) 9.
[2] R. von Helmolt, U. Eberle, Journal of Power Sources 165 (2007) 833.
[3] G.J.K. Acres, Journal of Power Sources 100 (2001) 60.
[4] P. Costamagna, S. Srinivasan, Journal of Power Sources 102 (2001) 253.
[5] R. Borup, J. Meyers, B. Pivovar, Y.S. Kim, R. Mukundan, N. Garland, D. Myers, M. Wilson, F. Garzon, D. Wood, K. Zelenay, K. More, T. Stroh, J. Zawodzinski, J.E. Boncella, M. McGrath, K. Inaba, M. Miyatake, K. Hori, Z. Ota, S. Ogumi, A. Miyata, Z. Nishikata, Y. Siroma, K. Uchimoto, K. Yasuda, i. Kimijima, N. Iwashita, Chemical Review 107 (10) (2007) 3904.
[6] B. Smitha, S. Sridhar, A.A. Khan, Journal of Membrane Science 259 (2005) 10.
[7] O. Savadogo, Journal of Power Sources 127 (2004) 135.
[8] J. Roziere, D.J. Jones, Annual Review of Materials Research 2003 (33) (2003) 503.
[9] M. Hogarth, G.A. Hards, Platinum Metals Review 40 (4) (1996) 150.
[10] V. Neburchilov, J. Martin, H. Wang, J. Zhang, Journal of Power Sources 169 (2007) 221.
[11] A.S. Arico, S. Srinivasan, V. Antonucci, Fuel Cells 1 (2) (2001) 133.
[12] L. Jorissen, V. Gogel, J. Kerres, J. Garche, Journal of Power Sources 105 (2002) 267.
[13] V.S. Silva, A. Mendes, L.M. Madeira, S. Nunes, Journal of Membrane Science 276 (2006) 126.
[14] L. Gubler, D. Kramer, J. Belack, O. Unsal, T.J. Schmidt, G. Scherer, Journal of the Electrochemical Society 154 (9) (2007) B981.
[15] N.W. Deluca, Y.A. Elabd, Journal of Polymer Science: Part B: Polymer Physics 44 (2006) 2201.
[16] D. Yamamoto, H. Munakata, K. Kanamura, Journal of the Electrochemical Society 155 (3) (2008) B303.
[17] J.-T. Wang, J.S. Wainright, R.F. Savinell, M. Litt, Journal of Applied Electrochemistry 26 (1996) 751.
[18] R. Wycisk, J.K. Lee, P.N. Pintauro, Journal of the Electrochemical Society 152 (5) (2005) A892.
[19] C.H. Fujimoto, M.A. Hickner, C. Cornelius, D.A. Loy, Macromolecules 38 (2005) 5010.
[20] M.A. Hickner, C.H. Fujimoto, C.J. Cornelius, Polymer 47 (2006) 4238.
[21] U. Kumar, T.X. Neenan, Macromolecules 28 (1995) 124.
[22] M. Sankir, Y.S. Kim, B.S. Pivovar, J.E. McGrath, Journal of Membrane Science 299 (2007) 8.
[23] J. Peckham, J. Schimeisser, M. Rodgers, S. Holdcroft, Journal of Materials Chemistry 17 (2007) 3255.
[24] K.D. Kreuer, Journal of Membrane Science 185 (2001) 29.
[25] T. Zawodzinski, C. Derouin, S. Radzinski, R. Sherman, V.T. Smith, T.E. Springer, S. Gottesfeld, Journal of the Electrochemical Society 140 (4) (1993) 1041.
[26] Y. Li, A. Roy, A.S. Badami, M. Hill, J. Yang, S. Dunn, J.E. McGrath, Journal of Power Sources 172 (2007) 30.
[27] M.L. Einsla, Y.S. Kim, M. Hawley, H. Lee, J.E. McGrath, B. Liu, M.D. Guiver, B.S. Pivovar, Chemistry of Materials 20 (17) (2008) 5636.
[28] Z. Siroma, N. Fujiwara, T. Ioroi, S. Yamazaki, K. Yasuda, Y. Miyazaki, Journal of Power Sources 126 (2004) 41.
[29] Y.A. Elabd, E. Napadensky, C.W. Walker, K.I. Winey, Macromolecules 39 (1) (2006) 399.
[30] G.E. Cise, L.S. Melnicki, E.J. Rudd, Journal of the Electrochemical Society 125 (3) (1978) C162.
[31] V.D. Grebenyuk, O.V. Grebenyuk, Russian Journal of Electrochemistry 38 (8) (2002) 806.
[32] T. Mohammadi, M. Skyllas-Kazocos, Journal of Applied Electrochemistry 27 (1997) 153.
[33] D. Chu, R. Jiang, Electrochimica Acta 51 (2006) 5829.
[34] V.S. Silva, S. Weisshaar, R. Reissner, B. Ruffmann, S. Vetter, A. Mendes, L.M. Madeira, S. Nunes, Journal of Power Sources 145 (2005) 485.